Spin and radiation in intense laser fields

M. W. Walser,* D. J. Urbach,† K. Z. Hatsagortsyan,‡ S. X. Hu,§ and C. H. Keitel‖
Theoretische Quantendynamik, Fakultät für Physik, Universität Freiburg, Hermann-Herder-Straße 3, D-79104 Freiburg, Germany
(Received 26 September 2001; published 4 April 2002)

The spin dynamics and its reaction on the particle motion are investigated for free and bound electrons in intense linearly polarized laser fields. Employing both classical and quantum treatments we analytically evaluate the spin oscillation of free electrons in intense laser fields and indicate the effect of spin-orbit coupling on the motion of the electron. In Mott scattering an estimation for the spin oscillation is derived. In intense laser ion dynamics spin signatures are studied in detail with emphasis on high-order harmonic generation in the tunneling regime. First- and second-order calculations in the ratio of electron velocity and the speed of light show spin signatures in the radiation spectrum and spin-orbit effects in the electron polarization.

DOI: 10.1103/PhysRevA.65.043410 PACS number(s): 32.80.Rm, 42.50.Hz, 33.40.+f

I. INTRODUCTION

The spin degree of freedom is always associated with a free or bound electron but it may not always be necessary to include it in describing the electron dynamics. In the theoretical description of electrons and atoms the spin does only play a minor role for the intensity regime up to at about 10^{16} W/cm^2 for near-optical laser pulses [1]. This results from the fact that the magnetic-field component of the laser pulse does not induce substantial spin dynamics and spin-orbit coupling. Thus, the electron motion is altered only a little as compared to the dynamics via the acceleration induced by the electric-field components of the laser field and the ionic core. In high-order harmonic generation via intense laser-atom interaction, coherent light has been generated in atoms up into the soft x-ray regime [2–4] with modestly intense laser fields. Involving multiply charged ions [5–7] or free electrons [8–11] in laser field pulses beyond 10^{16} W/cm^2, there is clear hope for achieving more energetic x rays and with this the need for understanding the role of the spin in this regime of relativistic interaction.

There has been considerable effort for several years in understanding the relativistic dynamics of electrons [8–11] and atoms [12–20] in such intense laser fields that the velocity of the electrons becomes non-negligible compared to that of light. The role of the magnetic-field component and higher-order relativistic effects was studied with respect to ionization and stabilization [12] and to harmonic generation [13]. Quantum relativistic treatments with spin via the Dirac equation were carried out for bound electrons [14], scattering scenarios [15,16], and related situations [17] in high-power lasers fields though excluding the tunneling regime of interest for high-order harmonic generation. A disadvantage of the full Dirac theory is the lack of the precise isolated role of spin-induced dynamics as compared to all the other relativistic influences such as the mass shift or *Zitterbewegung*. Thus, there is considerable benefit in studying expansions of the Dirac equation in the ratio of electron velocity with respect to that of light where all relativistic effects may be associated with different terms in the Hamiltonian. Corresponding calculations for laser-atom interaction have been carried out to first order via the Pauli equation [18] and up to second order including spin-orbit coupling [19] with clear spin signatures pointed out in the latter case.

In this paper, spin dynamics and spin-induced motions are investigated in the tunneling regime of weakly relativistic laser-ion interaction. Clear spin signatures are both pointed out in the high-order harmonic generation spectrum and in the polarization of the spin itself. The same properties are also evaluated for free electrons in intense laser fields based on classical and quantum mechanical treatments, i.e., including quantitative evaluations of the deviations of the free electron dynamics with spin as compared to that without. Finally for completeness we estimate explicitely the spin dynamics for Mott scattering showing spin flips for strong electron-ion interaction. Our calculations imply that for optical laser intensities above 10^{16} W/cm^2 spin-induced forces begin not to be insignificant anymore for dynamics and radiation while they may become rather large above 10^{20} W/cm^2.

The paper is organized as follows: In Sec. II A, the dynamics of the spin degree of freedom is evaluated for free electrons in an intense laser field, first classically and then within the conventional quantum description of the spin. This is followed by an investigation of spin-induced dynamics of laser-driven electrons in Sec. II B with the main calculations relegated to the Appendix. In Sec. III, we evaluate the evolution of the spin of a laser-driven electron on a hyperbolic trajectory around an ionic core. Finally in the main part in Sec. IV, the role of the spin for multiply charged single-electron ions is studied in intense laser fields with emphasis on the tunneling regime. In Sec. IV A, we employ the Pauli equation to investigate the spin dynamics and the spectral components of the high-order harmonic spectra arising from both spin-up and spin-down components of the wave func-

*Present address: Institut für Photonik, Technische Universität Wien, Gusshausstrasse 27/387, A-1040 Wien, Austria.
†Electronic address: David.Urbach@gwf.admin.ch
‡Permanent address: Department of Theoretical Physics, Yerevan State University, A. Manoukian Street 1, 375025 Yerevan, Armenia.
§Present address: Department of Physics and Astronomy, University of Nebraska–Lincoln, Lincoln, NE 68588-0111.
‖Electronic address: keitel@uni-freiburg.de

tion. In Sec. IV B, second-order relativistic corrections are studied in high-order harmonic generation (HHG) and spin dynamics, with emphasis on the harmonic linewidths and the position of the cutoff. In Sec. IV C, the direct radiation via spin oscillations is evaluated and in Sec. IV D, analytical estimations are presented to evaluate when spin effects may become large. We end with conclusions.

II. FREE SPIN DYNAMICS AND SPIN REACTION

In this section, we consider the role of the spin degree of freedom in the dynamics of a free electron in an intense laser field. The problem may be investigated in two parts: The evolution of the spin as investigated in the first subsection and the reaction of the evolving spin on the motion of the particle itself in the subsection afterwards. Astonishingly, spin precession may be modeled remarkably well within the classical picture of representing the spin by an angular momentum [21]. This is confirmed also by the fact that even the high-precision experiments of the anomalous moment of the electron or the muon take advantage in their interpretation of classical equations [22]. As a consequence a large fraction of our considerations will be classical even though in each case at least an approximate quantum analysis will follow to essentially confirm the classical results.

A. Spin dynamics

Free electron dynamics in intense laser physics is essentially classical [8], so that the first two parts of the subsection will treat subsequently the nonrelativistic and the relativistic situations of a laser-driven electron with magnetic moment. The corresponding quantum treatment of the spin associated to the particle will be shown to lead to spin oscillation dynamics being identical to the classical predictions in the nonrelativistic case in the third part of the subsection.

1. Nonrelativistic classical dynamics

The nonrelativistic equation of motion of a classical particle with charge q, mass m, and velocity $v=(v_x,v_y,v_z)$ in a linearly polarized plane laser field with polarization x, magnetic-field y, and laser propagation axis z reads

$$m\frac{d\boldsymbol{v}}{dt}=q\left(\boldsymbol{E}+\frac{\boldsymbol{v}}{c}\times\boldsymbol{B}\right), \tag{1}$$

with laser electric-field $\boldsymbol{E}=(E_0\cos(\omega t-kz),0,0)$, laser magnetic-field $\boldsymbol{B}=(0,E_0\cos(\omega t-kz),0)$, angular frequency ω, $k=\omega/c$, and c is the velocity of light. We introduce the eigen-time-parameter $\tau:=t-z/c$ and transform Eq. (1),

$$m\frac{dv_x}{d\tau}=qE_0\cos(\omega\tau),$$

$$m\frac{dv_y}{d\tau}=0,$$

$$m\frac{dv_z}{d\tau}=q\frac{1}{c}\frac{dx}{d\tau}E_0\cos(\omega\tau). \tag{2}$$

If the particle is at rest in the origin at the beginning, the solution of Eq. (2) reads

$$v_x=v_0\sin(\omega\tau),\quad v_y=0,$$

$$v_z=c\left(1-\sqrt{1-\frac{v_0^2}{c^2}\sin(w\tau)^2}\right), \tag{3}$$

with $v_0=qE_0/m\omega$. In units of v_0/ω the trajectory in the x-z plane is implicitly given by

$$\left(\frac{c}{v_0}\ln\left[\frac{1+v_0/c}{\sqrt{1-(v_0^2/c^2)\sin(\eta)^2}+(v_0/c)\cos(\eta)}\right],\right.$$

$$\left.\frac{c}{v_0}\left[F\left(\eta,\frac{v_0}{c}\right)-\eta\right]\right),\quad \eta\in\mathbb{R}, \tag{4}$$

where $F(\eta,v_0/c)$ is the elliptic integral of the first kind [23] and $\eta=\omega\tau$ is the free argument of the parametric function. While the particle is moving according to Eq. (3), its spin changes. Starting point of a classical description of spin dynamics is the equation of Larmor precession [24] of the magnetic moment $\boldsymbol{m}=\kappa\boldsymbol{s}$, $\kappa=q/mc$ of a particle with spin $\boldsymbol{s}$,

$$\frac{d\boldsymbol{s}}{dt}=\kappa\boldsymbol{s}\times\left(\boldsymbol{B}-\frac{\boldsymbol{v}}{c}\times\boldsymbol{E}\right),\quad \boldsymbol{s}^2=\frac{\hbar^2}{4}. \tag{5}$$

Making the ansatz $\boldsymbol{s}=(s\cos\theta,0,s\sin\theta)$, $s=\hbar/2$, we then derive the equation $d\theta/d\tau=\kappa E_0\cos(\omega\tau)$ for θ and thus the change of the angle $\Delta\theta$ with

$$\Delta\theta(\tau)=\theta(\tau)-\theta_0=\frac{v_0}{c}\sin(\omega\tau), \tag{6}$$

where θ_0 denotes the initial orientation of the spin.

2. Relativistic classical dynamics

The fully relativistic classical motion for the same situation as in the previous subsection suffices the equation

$$m\frac{d\boldsymbol{u}}{dt}=q\left(\boldsymbol{E}+\frac{\boldsymbol{v}}{c}\times\boldsymbol{B}\right),\quad \frac{d\varepsilon}{dt}=q\boldsymbol{v}\boldsymbol{E}, \tag{7}$$

with the three-velocity $\boldsymbol{u}=\gamma\boldsymbol{v}$, the energy $\mathcal{E}=\gamma mc^2$ and $\gamma=(1-v^2/c^2)^{-1/2}$. Subtracting the equation for u_z from the equation for $\mathcal{E}$ and integration over t we obtain, in our situation, the equivalence of the proper time τ with $t-z/c$, i.e., $\tau=t-z/c$. Using this, we solve Eq. (7),

$$u_x(\tau)=v_0\sin(\omega\tau),\quad u_y(\tau)=0,\quad u_z(\tau)=\frac{1}{2}\frac{v_0^2}{c}\sin(\omega\tau)^2,$$

$$\gamma(\tau)=1+\frac{1}{2}\frac{v_0^2}{c^2}\sin(\omega\tau)^2. \tag{8}$$

Thus, in units v_0/ω the trajectory in the x-z plane is

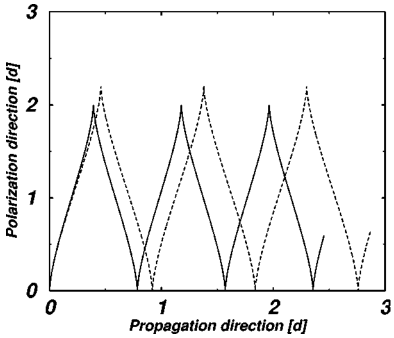

FIG. 1. A fraction of a classical nonrelativitic (dashed) and relativistic (solid) trajectory in units of $d=v_0/\omega$ according to Eqs. (4) and (9), respectively, with $v_0/c=0.5$. For the same value of η the relativistically moving particle has covered a smaller distance in the z direction than the nonrelativistic one. Quantum features, as in particular the spin, will further alter the motion of the particle. Quantifying and understanding those represent the major task of this paper.

$$\left(1-\cos(\eta),\frac{1}{4}\frac{v_0}{c}\left[\eta-\frac{1}{2}\sin(2\eta)\right]\right), \quad \eta\in\mathbb{R}, \tag{9}$$

as sketched in Fig. 1 for typical parameters. The relativistic equation describing the spin precession is the generalization of Eq. (5), Thomas's equation [24]

$$\frac{d\boldsymbol{s}}{dt}=\kappa\boldsymbol{s}\times\left(\frac{1}{\gamma}\boldsymbol{B}-\frac{1}{1+\gamma}\frac{\boldsymbol{v}}{c}\times\boldsymbol{E}\right), \tag{10}$$

Making again the ansatz $\boldsymbol{s}=(s\cos\theta,0,s\sin\theta)$ we get $d\theta/d\tau=\kappa[1-u_z/c(1+\gamma)]E_0\cos(\omega\tau)$ with the solution

$$\Delta\theta(\tau)=\theta(\tau)-\theta_0=2\arctan\left[\frac{1}{2}\frac{v_0}{c}\sin(\omega\tau)\right]. \tag{11}$$

In the case of small velocities, $v_0/c\ll 1$, Eq. (11) becomes Eq. (6).

3. Quantum dynamics

The nonrelativistic Hamilton operator of the Schrödinger equation which describes the time evolution of the spin of a particle moving classically according to Eq. (3) reads

$$\begin{aligned}H&=-\frac{\kappa\hbar}{2}\left(\boldsymbol{B}-\frac{\boldsymbol{v}}{c}\times\boldsymbol{E}\right)\boldsymbol{\sigma}\\&=-\frac{\kappa\hbar}{2}E_0\cos(\omega\tau)\left(1-\frac{v_z}{c}\right)\sigma_y,\end{aligned} \tag{12}$$

where $\boldsymbol{\sigma}=(\sigma_x,\sigma_y,\sigma_z)$ is the vector of the Pauli matrices. We denote the eigenvectors of σ_y with $|+\rangle_y$ and $|-\rangle_y$. We have described the spin degree within the conventional quantum treatment, however we will evaluate the particle dynamics itself, and with this τ in above equation, classically. The ansatz $\Psi=a|+\rangle_y+b|-\rangle_y$, $|a|^2+|b|^2=1$, and $c\ll v_z$ lead to the equations

$$\frac{da}{d\tau}=i\frac{\kappa E_0}{2}\cos(\omega\tau)a, \quad \frac{db}{d\tau}=-i\frac{\kappa E_0}{2}\cos(\omega\tau)b \tag{13}$$

with the solutions

$$\begin{aligned}a(\tau)&=a_0\exp\left[i\frac{1}{2}\frac{v_0}{c}\sin(\omega\tau)\right],\\ b(\tau)&=b_0\exp\left[-i\frac{1}{2}\frac{v_0}{c}\sin(\omega\tau)\right]\end{aligned} \tag{14}$$

for any variable a_0 and b_0 with normalization $|a_0|^2+|b_0|^2=1$. When we set the velocity operators v_y and v_z equal to zero, we mean that the corresponding expectation values are negligible for the parameter regime of interest. The expectation value of the spin operator $(\hbar/2)\boldsymbol{\sigma}$ with respect to the special initial state

$$\begin{aligned}\Psi_0=&\exp[i(\theta_0/2-\pi/4)]/\sqrt{2}|+\rangle_y\\&+\exp[-i(\theta_0/2-\pi/4)]/\sqrt{2}|-\rangle_y\end{aligned} \tag{15}$$

is $(\hbar/2)\langle\Psi_0|\boldsymbol{\sigma}|\Psi_0\rangle=(\hbar/2)(\cos\theta_0,0,\sin\theta_0)=(s\cos\theta_0,0,s\sin\theta_0)$, where we have used the following general relations for $\Psi=a|+\rangle_y+b|-\rangle_y$:

$$\begin{aligned}\langle\Psi|\sigma_x|\Psi\rangle&=2\,\mathrm{Im}(a^*b),\\ \langle\Psi|\sigma_y|\Psi\rangle&=|a|^2-|b|^2,\\ \langle\Psi|\sigma_z|\Psi\rangle&=2\,\mathrm{Re}(a^*b).\end{aligned} \tag{16}$$

The motivation of the particular choice of the state Ψ_0 was to match the corresponding classical initial state in Sec. II A 1. Consequently, we are able to compare the results via classical and quantum treatments sensibly. Its time evolution $\Psi(\tau)$ is determined by Eq. (14). The expectation value of the spin operator with respect to $\Psi(\tau)$ is therefore

$$\frac{\hbar}{2}\langle\Psi(\tau)|\boldsymbol{\sigma}|\Psi(\tau)\rangle=(s\cos\theta(\tau),0,s\sin\theta(\tau)), \tag{17}$$

which coincides with the classical result. Second- and higher-order relativistic effects involve the reaction of the spin on the electron dynamics and will be the subject of the following subsection.

B. Spin-induced dynamics

We now turn to the spin reaction of free electrons in intense laser fields on their own dynamics. The calculation to be shown in detail in the Appendix indicates that those motions are small with present-day laser parameters but not necessarily on the scale of the corresponding dynamics without the spin. Without the presence of the spin there is no force on the electron in the direction of the magnetic field direction of the linearly polarized laser field. However, with spin we find a laser and spin-induced velocity $v_y(\eta)$

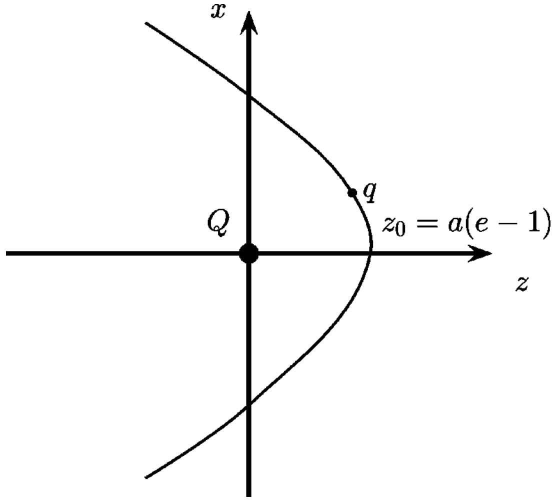

FIG. 2. Schematic scheme for the scattering process of a spinning electron at a positive ion along a hyperbolic trajectory. The ion with effective charge Q is situated in the focus of the hyperbola with semiaxis a and eccentricity e.

$$v_y(\eta) = -\frac{q\hbar E_0}{2m^2c^2}\cos(\eta) = -\frac{cE_0}{2E_c}\cos(\eta), \tag{18}$$

where $E_c = m^2c^3/(q\hbar)$ is the critical-field strength. Thus, electric-field strengths much higher than available today are necessary to reach spin-induced velocities comparable to that of light. Obviously though those velocities are still large as compared to zero which would be the velocity of an initially resting spinless classical electron in the magnetic-field direction of a linearly polarized laser field. Finally, Eq. (18) shows that quantum electrodynamics may alter spin-induced velocities.

III. THE SPIN IN ELECTRON-ION SCATTERING

Before the bound dynamics of a spinning electron we consider the scattering process in this section. Spin-induced forces for Mott scattering with high-laser intensities have already been evaluated within elaborate Dirac treatments [15] and discussed recently via comparing a Dirac and Klein-Gordon approach [16]. We therefore only restrict ourselves to estimate the dynamics of the spin degree of freedom within an approximate treatment and put forward a quite simple and intuitive result.

In order to obtain an idea of how the spin of a particle with charge $q<0$ changes when flying by an ion with $Q>0$ we investigate the situation of a particle passing the ion on an hyperbolic trajectory introducing the parameters a,e,z_0 (see Fig. 2). As in the previous section, the starting point is the equation

$$\frac{d\boldsymbol{s}}{dt} = \kappa\boldsymbol{s}\times\boldsymbol{B}, \quad \boldsymbol{s}^2 = \frac{\hbar^2}{4}. \tag{19}$$

The magnetic-field $\boldsymbol{B}$ in the rest frame of the particle in the nonrelativistic case is

$$\boldsymbol{B} = -\frac{\boldsymbol{v}}{c}\times\boldsymbol{E} = \frac{\boldsymbol{v}}{c}\times\boldsymbol{\nabla}\frac{Q}{r} = -\frac{Q}{cr^2}\boldsymbol{v}\times\boldsymbol{e}_r. \tag{20}$$

$\boldsymbol{B}$ only has a y component, $B_y = (Q/cr^3)(\dot{x}z - \dot{z}x)$. The ansatz $\boldsymbol{s} = (s\cos\theta, 0, s\sin\theta)$, where $s = \hbar/2$, together with Eq. (19) leads to

$$\theta = \frac{\kappa Q}{c}\int_{t_0}^{t}\frac{\dot{x}z - \dot{z}x}{r^3}ds. \tag{21}$$

From classical mechanics we know that the angular momentum $L_y = m(\dot{x}z - \dot{z}x)$ is a constant of motion. Using the parameter auxiliary ξ we can express the distance r from the origin and the time t as follows [25]:

$$r = a(e\cosh\xi - 1),$$
$$t = \sqrt{\frac{ma^3}{\alpha}}(e\sinh\xi - \xi), \quad \alpha = -qQ. \tag{22}$$

We set $t_0 = 0$, $r(t_0) = r_{\min} = z_0$, transform Eq. (21) and get

$$\frac{\Delta\theta}{2} = \frac{\kappa Q\sqrt{ma^3/\alpha}L_y}{mca^3}\int_0^{\xi}(e\cosh s - 1)^{-2}ds$$
$$= \frac{\kappa Q\sqrt{ma^3/\alpha}L_y}{mca^3}\left[\frac{2\arctan[(e+1)\tanh(\xi/2)/\sqrt{e^2-1}]}{(e^2-1)^{3/2}} + \frac{e\sinh(\xi)}{(e^2-1)(e\cosh\xi - 1)}\right]. \tag{23}$$

If ξ and thus r approaches infinity this expression simplifies to

$$\frac{\Delta\theta}{2} = \frac{\kappa Q\sqrt{ma^3/\alpha}L_y}{mca^3}\left[\frac{2\arctan[(e+1)/\sqrt{e^2-1}]}{(e^2-1)^{3/2}} + \frac{1}{e^2-1}\right]. \tag{24}$$

For the energy of the particle $\mathcal{E}$ the relation

$$\mathcal{E} = \frac{mv^2}{2} - \frac{\alpha}{r} = \frac{\alpha}{2a} \tag{25}$$

holds [25]. We assume v_0 to be the velocity when the particle passes the z axis $[x=0, \quad z=z_0=a(e-1)]$, so that $L_y/m = z_0 v_0$. We express all quantities in Eq. (24) by e and z_0

$$\frac{\Delta\theta}{2} = \frac{\kappa Q}{c}\frac{(e-1)\sqrt{e^2-1}}{z_0}\left[\frac{2\arctan[(e+1)/\sqrt{e^2-1}]}{(e^2-1)^{3/2}} + \frac{1}{e^2-1}\right]. \tag{26}$$

If e approaches infinity, the hyperbola becomes a straight line and the spin makes the finite jump

$$\Delta\theta = \frac{2\kappa Q}{c z_0}. \tag{27}$$

This shows that the change of the spin is proportional to the charge of the ion Q and depends critically on the closest distance z_0 of the electron to the ion. A scaling in terms of the tiny classical electron radius $r_0 = e^2/mc^2$ leads to $\Delta\theta = (2qQ/e^2)(r_0/z_0)$ and indicates in addition that a substantial turn of the spin occurs only for electrons virtually touching the ion.

IV. SPIN AND RADIATION IN LASER-DRIVEN BOUND IONIC SYSTEMS

In this section, we consider the role of the spin in bound-electron dynamics. In the so-called multiphoton regime where the force of the ionic core on the electron is mostly considerably larger than that of the laser field on the electron, spin effects due to spin-orbit coupling have recently been studied in detail [19]. When the laser field is the dominating force, the motion is essentially such that the electron dynamics is mostly free in the laser field as discussed Sec. II. Our interest in this section is directed to the remaining tunneling regime where both forces, i.e., from ion and laser field, may become comparable and where parts of the bound-electron wave packet may leave the ion via tunneling. To be concrete, we investigate the dynamics of a multiply charged hydrogenic ion with effective charge $Z=4$ in near-optical linearly polarized laser pulses with intensities of order 10^{16} to 10^{17} W/cm^2. The weakly relativistic interaction is appropriately described by the Hamiltonian arising from the expansion of the Dirac equation up to order $1/c^2$. While spin oscillations occur already in first order in $1/c$ as predicted by the Pauli equation, correction terms of order $1/c^2$ are necessary to describe the influence of the spin on dynamics and radiation of the electron. Parts of the electronic wave-packet tunnel through the potential barrier of the ionic core and when recombining are shown to give rise to kilo-electron-volt harmonics in the radiation field.

A. Bound spin dynamics and radiation

We now turn to the investigation of the dynamics of a charged ion with charge state $Z=4$ subjected to the field of a KrF laser (248 nm, 0.183 a.u.) with intensities 10^{16} to 10^{17} W/cm^2. We consider the Dirac equation up to first and second order in $1/c$. Up to first-order this leads to the Pauli equation. One may derive first-order relativistic correction terms to the Pauli equation, which corresponds to second-order terms in $1/c$, continuing the method which was used to obtain the Pauli equation [26]. As opposed to most nonrelativistic treatments we need to include at least two dimensions in the calculations as the magnetic-field component of the laser pulse may induce a significant drift in the laser propagation direction. There is a spin-induced acceleration in the magnetic-field direction, i.e., in the remaining third dimension, but its influence is small for the observables and the parameters of interest here. The main advantage of using this approximated form of the Dirac Hamiltonian in comparison to the full one is the possible isolation of the influence of each physical mechanism arising. In addition we are not limited numerically to use high-frequency lasers as necessary so far with the full Dirac equation [14,16,17].

The Hamilton operator H_1 up to order in $1/c$ for a bound electron in a electromagnetic field writes

$$H_1 = H_0 + H_{\mathrm{P}},$$

$$H_0 = \frac{1}{2m}\left(\boldsymbol{p} - \frac{e}{c}\boldsymbol{A}\right)^2 + V(x,z),$$

$$H_{\mathrm{P}} = -\frac{e\hbar}{2mc}\boldsymbol{\sigma}\boldsymbol{B}. \tag{28}$$

Here, $\boldsymbol{p} = (p_x, 0, p_z)$ is the two-dimensional momentum operator and $\boldsymbol{A}(t,z)$ is the vector potential of the laser field which is linearly polarized along the x axis and propagates in z direction. We consider the ion in the single active electron approximation [27]. It is well described by a soft-core potential [28] to model the Coulomb field experienced by the active electron with charge e, i.e.,

$$V(x,z) = -\frac{k}{\sqrt{s + x^2 + z^2}}. \tag{29}$$

The parameter k is a function of the effective number of positive charges Z as sensed by the electron, whereas s compensates for the effect of possible inner electrons and reduced distances of the electronic wave packet to the ionic core in two- rather than three-dimensional calculations. The parameters k and s may be adapted such that we obtain the correct ionization energy for the system of interest [19].

Thus, we have to solve the following equation, written in atomic units:

$$i\frac{\partial}{\partial t}\begin{bmatrix}\Psi_\uparrow(\boldsymbol{x},t)\\ \Psi_\downarrow(\boldsymbol{x},t)\end{bmatrix} = H_1\begin{bmatrix}\Psi_\uparrow(\boldsymbol{x},t)\\ \Psi_\downarrow(\boldsymbol{x},t)\end{bmatrix}. \tag{30}$$

The wave function has two components corresponding to spin-up and spin-down polarization of the electron. The spacial dependence of the vector potential indicates that the magnetic component of the laser field $\boldsymbol{B} = \boldsymbol{\nabla}\times\boldsymbol{A}(t,z) \neq 0$ is included and we do not carry out the dipole approximation. We choose $A_x(t,z)$ such that $\boldsymbol{E} = (E_x, 0, 0)$ and $\boldsymbol{B} = (0, B_y, 0)$ have the following form:

$$E_x(t,z) = B_y(t,z)$$
$$= \begin{cases} 0, & t - z/c \leqslant 0, \\ E_0\dfrac{t-z/c}{t_{\mathrm{on}}}\cos(\omega t - kz), & 0 \leqslant t - z/c \leqslant t_{\mathrm{on}}, \\ E_0\cos(\omega t - kz), & t_{\mathrm{on}} \leqslant t - z/c \leqslant t_{\mathrm{off}}. \end{cases} \tag{31}$$

E_0 and ω are the maximal amplitude of both fields and the angular frequency of the laser, respectively. Further, t_{on} is associated with the linear rising time of the laser pulse. After the turn-on phase the pulse is assumed to have a constant amplitude until time t_{off}. Obviously a realistic pulse will turn off afterwards smoothly, however for all observables of interest here this phase is of no interest and numerical calculations terminate at t_{off}.

Since the laser field is linearly polarized, the interaction term involves a term of the form $\boldsymbol{p}\cdot\boldsymbol{A}(t,z)/c=p_xA_x(t,z)/c$, which means that there is no coupling between momentum and coordinate space. Thus, we can apply the conventional split-operator algorithm [29,30] to solve the two-dimensional time-dependent matrix Eq. (30) via

$$\begin{bmatrix}\Psi_\uparrow(\boldsymbol{x},t+dt)\\ \Psi_\downarrow(\boldsymbol{x},t+dt)\end{bmatrix}=\exp(-idt\boldsymbol{p}^2/4)\times\exp[-idtA_x(t,z)p_x/c]\exp(-idtH_{\mathrm{P}})\times\exp\{-idt[A_x(t,z)^2/2c^2+V(x,z)]\}\times\exp(-idt\boldsymbol{p}^2/4)\begin{bmatrix}\Psi_\uparrow(\boldsymbol{x},t)\\ \Psi_\downarrow(\boldsymbol{x},t)\end{bmatrix}. \tag{32}$$

Here, dt denotes the time step. All exponential operators except $\exp(-idtH_{\mathrm{P}})$ are diagonal. Fourier transforming between the coordinate representation and momentum representation we apply the split evolution operator on the wave function. Consequently all derivatives can be transformed into multiplications with constants. The operator $\exp(-idtH_{\mathrm{P}})=\exp[-idt\sigma_yB_y(t,z)/2c]$ only contains the matrix σ_y and can be calculated explicitly

$$\exp(-idt\sigma_yB_y(t,z)/2c)=\begin{bmatrix}\cos[dtB_y(t,z)/2c] & -\sin[dtB_y(t,z)/2c]\\ \sin[dtB_y(t,z)/2c] & \cos[dtB_y(t,z)/2c]\end{bmatrix}. \tag{33}$$

We apply it on the wave function in the coordinate representation. Special care is needed regarding the interaction term $A_x(t,z)p_x$. Here we do the Fourier transformation only for the x coordinate because of the z coordinate dependence of the vector potential $A_x(t,z)$. Because of the splitting of the the total Hamiltonian in the exponent we introduce an error following the Baker-Hausdorff formula because the split terms do not commute generally. The error of this algorithm is of order $O(dt^3)$ between each time step [31]. Thus, a small time step ensures to get accurate results. We have not experienced any problems with numerical convergence in the regime of interest here.

From the numerical point of view we start with computing the eigenstates of the bound electron in the ionic core potential by using the spectral method [32]. Figure 3 shows the energy-level structure of the model hydrogenlike ion with $Z=4$. Choosing $k=10.7$ and $s=1$ we obtain the corresponding ground-state energy -8 a.u. along with the various eigenfunction (see Fig. 4). Note that it is not our purpose to present an exact quantitative model of the ionic level structure of an ionic system. We model single-electron ions with a soft core rather than a Coulomb potential and can adapt the ground-state energy by choosing k and s. In the intensity range where level structures are important we can only make qualitative statements for the dynamics. In the tunneling regime however where only the correct ground state is significant we can be quantitative as well.

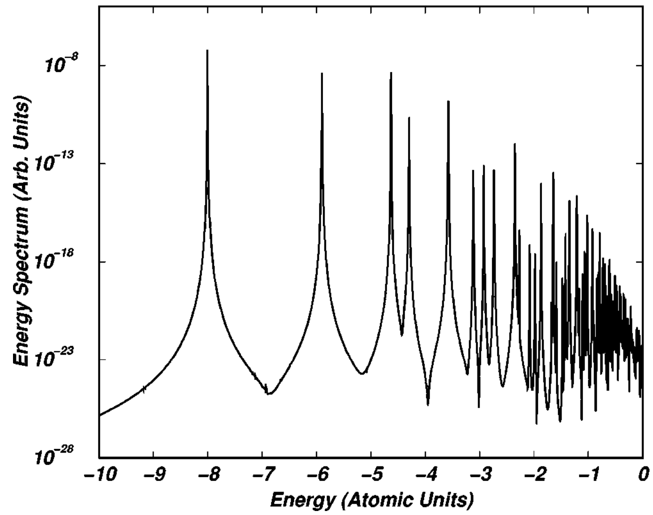

FIG. 3. The energy-level structure of a model multiply charged ion with charge state $Z=4$. The potential is described by a soft-core model, i.e., $V=-k/\sqrt{s+x^2+z^2}$ with $k=10.7$ and $s=1$ and the ground state energy is -8 a.u.

After the turn on of the laser the system develops from the ground state ($\Psi_\uparrow=$ground state, $\Psi_\downarrow=0$) and we use the split-operator algorithm to solve Eq. (30). In Fig. 5 we have displayed the expection value of $\Psi_\downarrow$ as a function of time for an electron polarized initially in spin-up orientation. Note the expected oscillation with twice the laser frequency and similar to the relativistic multiphoton regime in [19] the complete return of the expectation value to the original orientation. The latter feature will change once spin-orbit coupling is included in the next subsection.

With the knowledge of the time-dependent wave function we are in the position to calculate the expectation value of any observable $\mathcal{O}$:

$$\langle\mathcal{O}(t)\rangle=\int dx\int dz[\Psi_\uparrow^*(x,z,t),\Psi_\downarrow^*(x,z,t)]\mathcal{O}(x,z,t)\times\begin{bmatrix}\Psi_\uparrow(x,z,t)\\ \Psi_\downarrow(x,z,t)\end{bmatrix}. \tag{34}$$

Since we intend to calculate the radiation spectrum we are in particular interested in the acceleration in the polarization direction $a_x(t)=\langle\ddot{x}\rangle$ and in the propagation direction $a_z(t)=\langle\ddot{z}\rangle$.

The radiation spectrum is generally given by a rather complex function of the accelerations and velocities in all spatial directions [24]. For simplicity we here restrict ourself to the observation direction perpendicular to the plane of

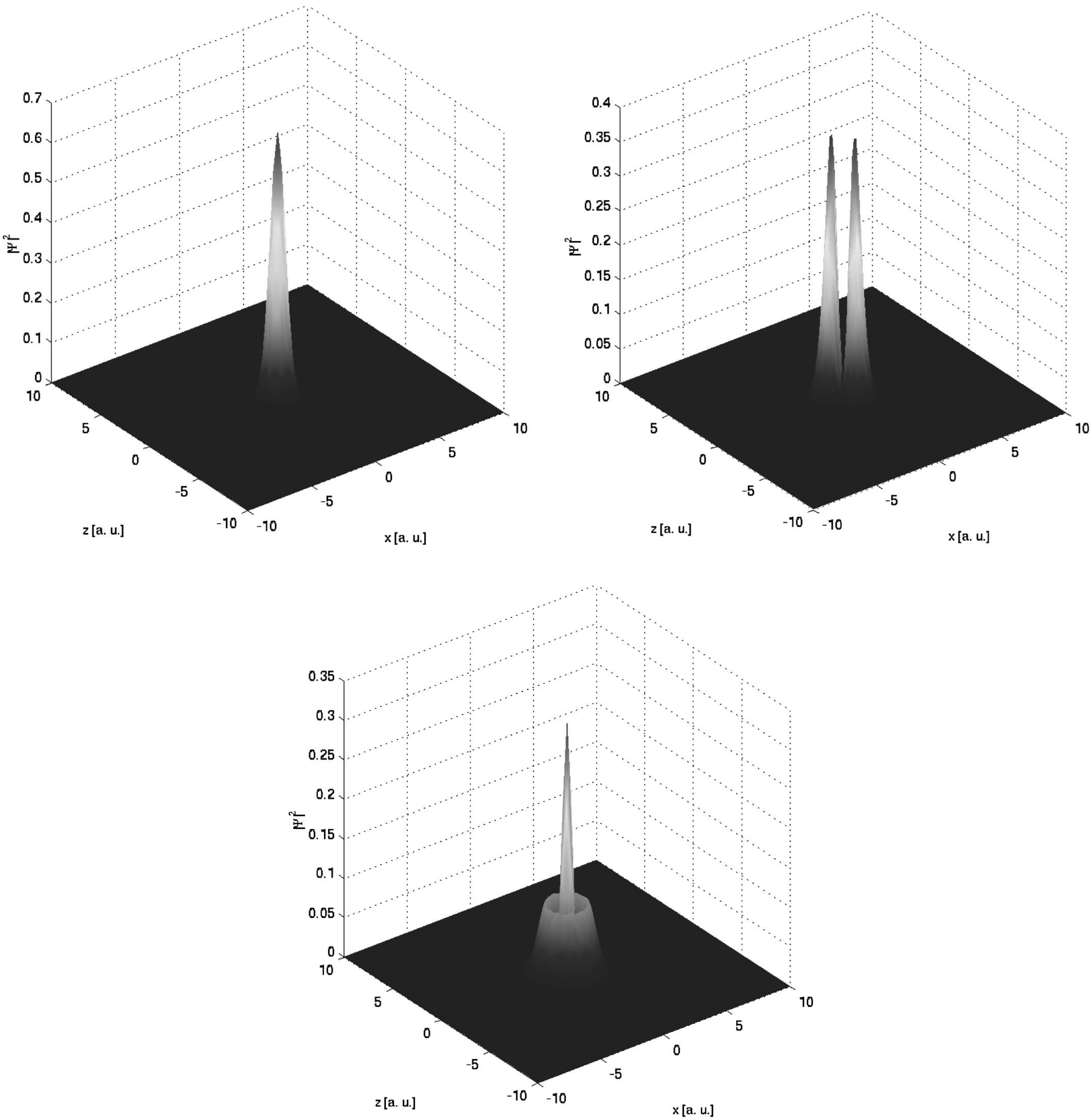

FIG. 4. The probability distribution of the electronic wave packets according to the potential $V=-k/\sqrt{s+x^2+z^2}$ with parameters indicated in Fig. 3: ground state (top), first (middle) and second excited state (bottom).

motion, i.e., to the y direction. The dominating part of the radiation spectrum in the weakly relativistic regime is polarized in the polarization direction of the laser field. In the far-field spectrum this is proportional to the squared Fourier transform of the acceleration $a_x(t)$. Furthermore, we study the less intense spectrum which is polarized in the laser propagation direction and governed by $a_z(t)$.

In connection with the Pauli equation [18] it is sufficient for $a_x(t)$ and $a_z(t)$ to consider the negative gradient of the potential

$$\langle\ddot{x}\rangle=-\left\langle\frac{\partial V(x,z)}{\partial x}\right\rangle,\quad \langle\ddot{z}\rangle=-\left\langle\frac{\partial V(x,z)}{\partial z}\right\rangle. \tag{35}$$

The acceleration due to the laser field can be neglected since it contributes mainly to the low harmonics, which are of little interest.

We are now in the position to investigate the influence of the spin on HHG, see Fig. 6. During tunneling, essentially free motion in the laser field and recollision with the core,

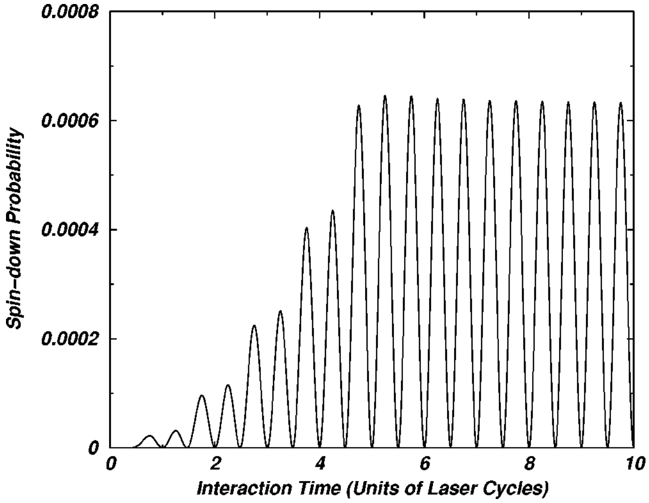

FIG. 5. The dynamics of the spin degree of freedom viewed via the population of the wave function with spin-down polarization. The initial electron is spin-up polarized. The laser parameters employed are $I=5.932\times10^{16}$ W/cm^2, $\lambda=248$ nm with a turn-on phase of five cycles and duration of the phase with constant amplitude of five cycles.

the spin degree of freedom will change and may alter the dynamics and radiation of the particle more or less significantly. Since the spin of the wave function has two components $\Psi_\uparrow$ and $\Psi_\downarrow$, both Fourier transforms of the corresponding two dipole accelerations $a_\uparrow^{\{x,z\}}(t)$ and $a_\downarrow^{\{x,z\}}(t)$ contribute to the total spectrum. This means that we have to calculate the Fourier transform of the following four accelerations:

$$a_\uparrow^j(t)=-\int\frac{\partial V(x,z)}{\partial j}|\Psi_\uparrow(x,z,t)|^2dxdz,$$

$$a_\downarrow^j(t)=-\int\frac{\partial V(x,z)}{\partial j}|\Psi_\downarrow(x,z,t)|^2dxdz, \tag{36}$$

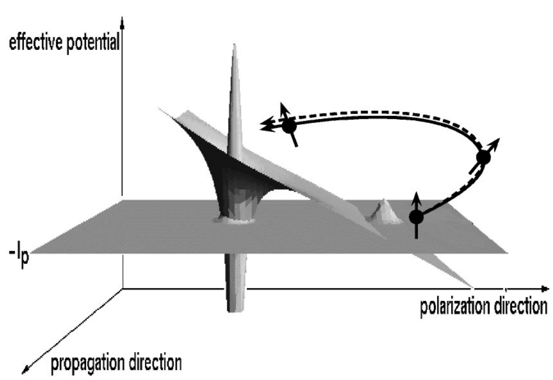

FIG. 6. Schematic diagram describing the dynamics of the tunneled fraction of the electron wave packet without (dashed line) and with spin degree of freedom (solid line) in an intense laser field. Shown as well is the tilted effective Coulomb potential of the ion and the laser field at maximal strength and inside is the ground-state wave packet with energy $-I_p$.

where $j\in\{x,z\}$. Spectra via the Pauli equation in the tunneling regime have been studied in [18]; the above expressions are employed later for a comparison with the corresponding relativistic results. In the following sections, we will also be able to evaluate the role of the spin on tunneling-recollision harmonics.

B. Spin-induced motion in bound-electron dynamics and radiation

In order to take spin reactions on the dynamics of the electron into account we have to include terms of order $1/c^2$ in the expansion of the Dirac Hamiltonian [26]. These terms are the leading relativistic mass shift term, the term describing the *zitterbewegung* and the term of the spin-orbit coupling. Our working Hamiltonian H_2 therefore reads

$$H_2=H_0+H_{\mathrm{P}}+H_{\mathrm{kin}}+H_{\mathrm{D}}+H_{\mathrm{SO}},$$

$$H_0=\frac{1}{2m}\left(\boldsymbol{p}-\frac{e}{c}\boldsymbol{A}\right)^2+V(x,z),$$

$$H_{\mathrm{P}}=-\frac{e\hbar}{2mc}\boldsymbol{\sigma}\cdot\boldsymbol{B},$$

$$H_{\mathrm{kin}}=-\frac{1}{8m^3c^2}\left(\boldsymbol{p}-\frac{e}{c}\boldsymbol{A}\right)^4,$$

$$H_{\mathrm{D}}=\frac{e\hbar^2}{8m^2c^2}\nabla\cdot\boldsymbol{E}',$$

$$H_{\mathrm{SO}}=-\frac{e\hbar}{4m^2c^2}\boldsymbol{\sigma}\left[\boldsymbol{E}'\times\left(\boldsymbol{p}-\frac{e}{c}\boldsymbol{A}\right)\right]. \tag{37}$$

$\boldsymbol{E}'$ stands for the sum of the electric field of the laser and the electric field of the core. The corresponding wave equation reads

$$i\frac{\partial}{\partial t}\begin{bmatrix}\Psi_\uparrow(\boldsymbol{x},t)\\ \Psi_\downarrow(\boldsymbol{x},t)\end{bmatrix}=H_2\begin{bmatrix}\Psi_\uparrow(\boldsymbol{x},t)\\ \Psi_\downarrow(\boldsymbol{x},t)\end{bmatrix}. \tag{38}$$

In order to solve Eq. (38) we have developed a variant of the split-operator algorithm. The temporal evolution of the wave function is given by

$$\begin{aligned}\begin{bmatrix}\Psi_\uparrow(\boldsymbol{x},t+dt)\\ \Psi_\downarrow(\boldsymbol{x},t+dt)\end{bmatrix}&=\exp[-idt(\boldsymbol{p}^2/4-p_x^4/16c^2)]\\ &\times\exp[-idt(A_x(t,z)p_x/c-A_x(t,z)p_x^3/2c^3\\ &-3A_x^2(t,z)p_x^2/4c^4-A_x^3(t,z)p_x/2c^5)]\\ &\times\exp(-idtH_{\mathrm{SO}})\exp(-idtH_{\mathrm{P}})\\ &\times\exp[-idt(A_x(t,z)^2/2c^2\\ &-A_x(t,z)^4/8c^6+V(x,z)+H_{\mathrm{D}})]\end{aligned}$$

$$\times \exp[-idt(\boldsymbol{p}^2/4-p_x^4/16c^2)]\begin{bmatrix}\Psi_\uparrow(\boldsymbol{x},t)\\ \Psi_\downarrow(\boldsymbol{x},t)\end{bmatrix}.$$

In Eq. (39) we have neglected all terms which include a factor p_z^2/c^2 since the influence of p_z on the wave function is one order in $1/c$ smaller than the influence of p_x. All exponential operators except $\exp(-idtH_{\mathrm{SO}})$ and $\exp(-idtH_{\mathrm{P}})$ are diagonal and we handle them as above. Also $\exp(-idtH_{\mathrm{P}})$ is handled as above. For the operator $\exp(-idtH_{\mathrm{SO}})$, which includes p_x and p_z, we carry out the Taylor expansion

$$\exp(-idtH_{\mathrm{SO}})=\mathbb{I}-iH_{\mathrm{SO}}dt-\frac{1}{2}H_{\mathrm{SO}}^2dt^2+iH_{\mathrm{SO}}^3dt^3+O(dt^4) \tag{40}$$

and apply it on the wave function in the coordinate representation.

Under the assumption of including relativistic corrections up to second order in $1/c$ it is not sufficient to consider the negative gradient of the potential only as in the previous case. From the classically relativistic equation of motion we rather find in the weakly relativistic limit (see also [19])

$$\ddot{x}=-\left(1+\frac{3}{2c^2}\frac{\partial^2}{\partial x^2}\right)\frac{\partial V(x,z)}{\partial x},$$

$$\ddot{z}=-\left(1+\frac{3}{2c^2}\frac{\partial^2}{\partial x^2}\right)\frac{\partial V(x,z)}{\partial z}. \tag{41}$$

Figure 7 shows the contributions of $\Psi_\uparrow$ and $\Psi_\downarrow$ to the spectrum, which are calculated using Eqs. (38) and (41). The high-frequency harmonics associated with the wave packet in spin-down orientation have a substantial coherence with respect to those without spin flip. In Fig. 7 (c) the harmonic spectrum emitted in the polarization direction is shown in the region of the cutoff. It compares the spectrum in two situations: turn-on phase 10 cycles (dashed line) and turn-on phase 15 cycles (solid line). In the second case the even harmonics are suppressed and the small odd ones can therefore be better distinguished. This effect can be enforced by prolonging the turn-on phase. We note that a spinless nonrelativistic calculation essentially delivers the same spectrum as the one shown without spin flip for those weakly relativistic parameters. This comparison could equally be done by comparing the results via the Dirac and Klein-Gordon equation, however with the identical small discrepancies in the weakly relativistic parameter regime as with our approach. Furthermore, we stress that the spectral features via the spin-down component are rather weak. This can be improved by increasing both the ion charges and the laser intensities into the relativistic regime. In this situation, however, the improvements of the coherence become less attractive.

In Fig. 8 the modulus of the difference of the spectrum which is polarized in the x direction and calculated via the Pauli Eq. (30) with the analogous one which is calculated via Eq. (38) is depicted. The figure shows that for an ion with charge state $Z=4$ the spin reaction on radiation is rather small in the tunneling regime. However, it is clearly notable already for such a moderately charged ion, especially for higher-laser intensities as shown in Fig. 8(b). A further significant effect of spin reaction is illustrated in Fig. 9, where the temporal evolution of $|\Psi_\downarrow|^2$ is viewed. Spin-orbit coupling causes an effective polarization of the spin, while without spin-orbit coupling the electron periodically returns to the initial polarization in complete spin-up configuration (compare with Fig. 5).

C. Pure spin radiation

Due to the linear polarization of the applied laser pulse at no more than weakly relativistic laser parameters, the emitted HHG radiation is also essentially linearly polarized in the direction of the electric field. Therefore, radiation with a substantial fraction of circular polarization may serve as an indicator for spin signatures in the HHG process. The main contribution to this radiation comes from the electron radiation due to spin oscillations. The calculation of the magnetic moment $\boldsymbol{\mu}$ of the electron responsible for the radiation yields

$$\boldsymbol{\mu}(t)=\frac{e\hbar}{2mc}\int \Psi^*(\boldsymbol{x},t)\boldsymbol{\sigma}\Psi(\boldsymbol{x},t)d^3x, \tag{42}$$

where we have to use the electron wave functions $\Psi=(\Psi_\uparrow,\Psi_\downarrow)$ via the solution of the second-order Eq. (38) including spin-orbit interaction, because it involves spin dynamics via the magnetic field of the ionic core sensed by the electron in its rest frame. The interaction with the ionic core is crucial for HHG in the tunneling regime via the tunneling-recollision mechanism. We are interested in this subsection in the oscillation of the magnetic moment in Eq. (42) and in particular in the radiation arising from it with differential intensity $dI_{\boldsymbol{n}\omega}$ per angular frequency $d\omega$ and spatial angle $d\Omega$

$$dI_{\boldsymbol{n}\omega}=\frac{\omega^4}{4\pi^2c^3}(\boldsymbol{\mu}_\omega\times\boldsymbol{n})^2d\Omega d\omega, \tag{43}$$

with $\boldsymbol{\mu}_\omega$ being the Fourier transform of $\boldsymbol{\mu}$ in Eq. (42). In Fig. 10, we have depicted the spin dynamics of a bound electron in the tunneling regime and the associated radiation. Oscillations of the magnetic moments are clearly visible of both considered components while nonlinear elements, however, are too small to be visible due to the moderately intense laser field employed. Since this radiation arises purely from spin oscillations it is a characteristic signature of the spin degree of freedom.

This radiation is rather weak in intensity, so that it may not be wise to detect it experimentally in the direction of the laser magnetic field as in Fig. 10 and in the previous subsections. The main part of the radiation via electron acceleration is polarized in the laser polarization direction and the fraction in the laser propagation direction is no more than one order of magnitude smaller for the weakly relativistic parameter regime employed in this article. The polarization of the spin radiation differs from that via the electron radiation in the laser magnetic-field direction but due to the large differ-

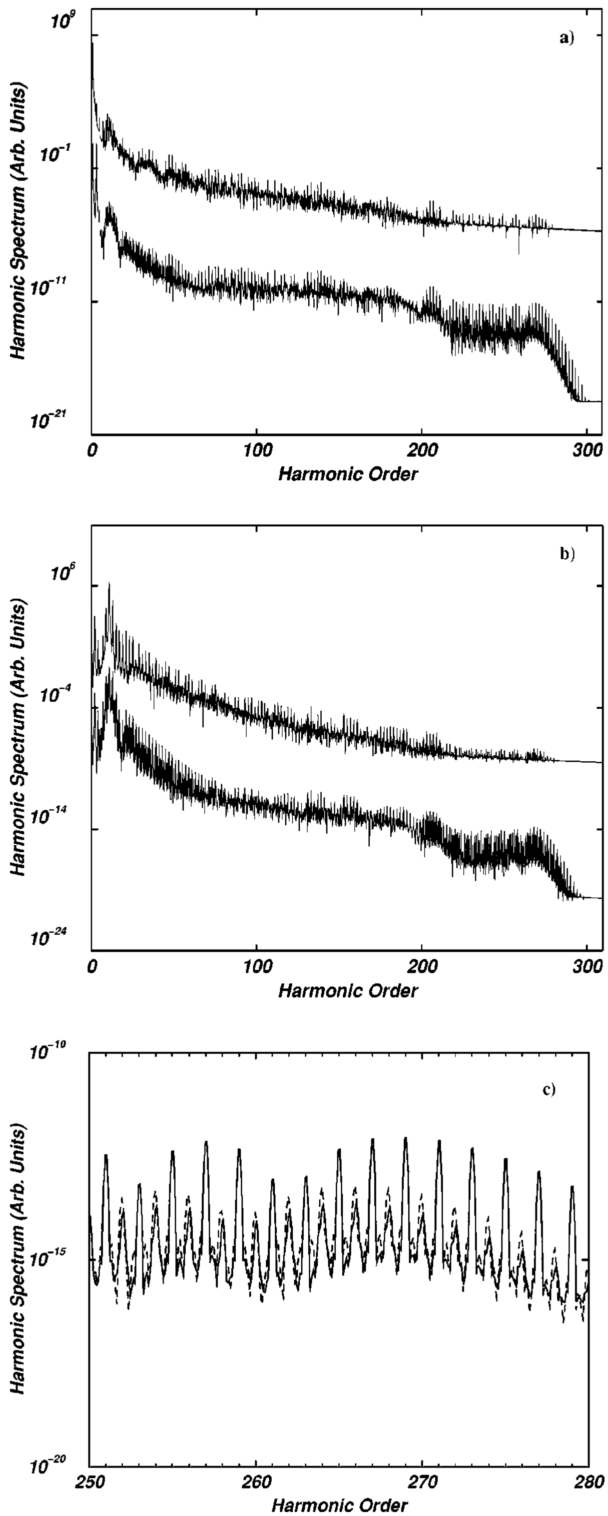

FIG. 7. The figure shows the contributions of $\Psi_{\uparrow}$ (upper curves) and $\Psi_{\downarrow}$ (lower curves) to the spectrum, which are calculated using Eqs. (38) and (41) with a polarization in the x direction (a) and a polarization in the z direction (b). The laser parameters employed are $I=5.932\times10^{16}$ W/cm^2 and $\lambda=248$ nm. The turn-on phase is ten cycles with a duration of the phase with constant amplitude of ten cycles. (c) Segment of the x-polarized spectrum in (a) in the cutoff regime via the spin-down component with respect to two situations: a turn-on phase of 10 cycles (dashed line) as in (a) and a turn-on phase of 15 cycles (solid line).

ence in intensities it is still likely to be challenging to isolate the pure spin radiation. The situation changes clearly when we observe in the direction of polarization of the laser field x. Then there will be none of the intense light polarized in the x direction and we may avoid radiation polarized in z direction entering the detector with a polarizer. There is no direct acceleration of the electron along the y axis via the laser pulse while the spin radiation in the x direction is purely polarized in the y direction. Thus, radiation polarized along this direction should be spin induced to a large extent.

D. Analytical estimations of spin-induced effects

In this subsection we aim to give rough estimations comparing spin induced effects with the other leading dynamical features. While spin effects become comparable to the other features in general only for rather high-laser intensities, we emphasize that this may be quite different for particular observables which tend to be very small already without the inclusion of the spin (such as dynamics and radiation polarized in the laser magnetic-field direction). Thus, the aim here is not to state when a spin correction becomes significant, but when it is even comparable in size to associated effects.

1. Direct spin radiation

We begin by estimating the order of magnitude of intensity of the radiation due to spin oscillations in Eq. (43) in relation to the dipole radiation without any differentiation on polarizations and directions of observation. The second-order derivative in time of the magnetic moment is $\ddot{\boldsymbol{\mu}}=-1/\hbar^2[H,[H,\boldsymbol{\mu}]]$, where H is the corresponding Hamiltonian, which may be reduced to

$$\ddot{\boldsymbol{\mu}}=\frac{e^3\hbar}{8m^3c^3}[(\boldsymbol{\sigma}\boldsymbol{F})\boldsymbol{F}-F^2\boldsymbol{\sigma}], \tag{44}$$

where $\boldsymbol{F}=\boldsymbol{B}+\boldsymbol{E}'\times(\boldsymbol{p}-e\boldsymbol{A}/c)/2mc$. With the aid of Eq. (44) we can estimate the absolute value of $|\ddot{\boldsymbol{\mu}}|$ to be $|\ddot{\boldsymbol{\mu}}^{P}|\approx(e^3\hbar/m^3c^3)B^2$ in the case without spin-orbit interaction, i.e., based on the Pauli equation with $H=H_1$. Here, B is the amplitude of the applied magnetic field of the laser pulse where we have neglected the sinusoidal spatial and temporal dependance for our order of magnitude estimation. Including the leading terms of spin-orbit coupling via the nucleus within the second-order differential dynamical Eqs. (38) and Eq. (37), i.e., $H=H_2$, we obtain instead: $|\ddot{\boldsymbol{\mu}}^{S}|\approx(e^3\hbar/m^3c^3)\times(B/mcr)|d\Phi/dr||\boldsymbol{L}\boldsymbol{\sigma}|\approx(e^2\hbar\omega/m^2c^2)\zeta(v/c)|d\Phi/dr|$, where Φ is the Coulomb potential. Introducing $\zeta=eE/mc\omega$ and comparing with the second derivative of the dipole moment $|\ddot{\boldsymbol{d}}|=(e^2/m)|d\Phi/dr|$ gives

$$\frac{|\ddot{\boldsymbol{\mu}}^{P}|}{|\ddot{\boldsymbol{d}}|}\approx\zeta\frac{\hbar\omega}{mc^2}\quad\text{and}\quad\frac{|\ddot{\boldsymbol{\mu}}^{S}|}{|\ddot{\boldsymbol{d}}|}\approx\zeta^2\frac{\hbar\omega}{mc^2}. \tag{45}$$

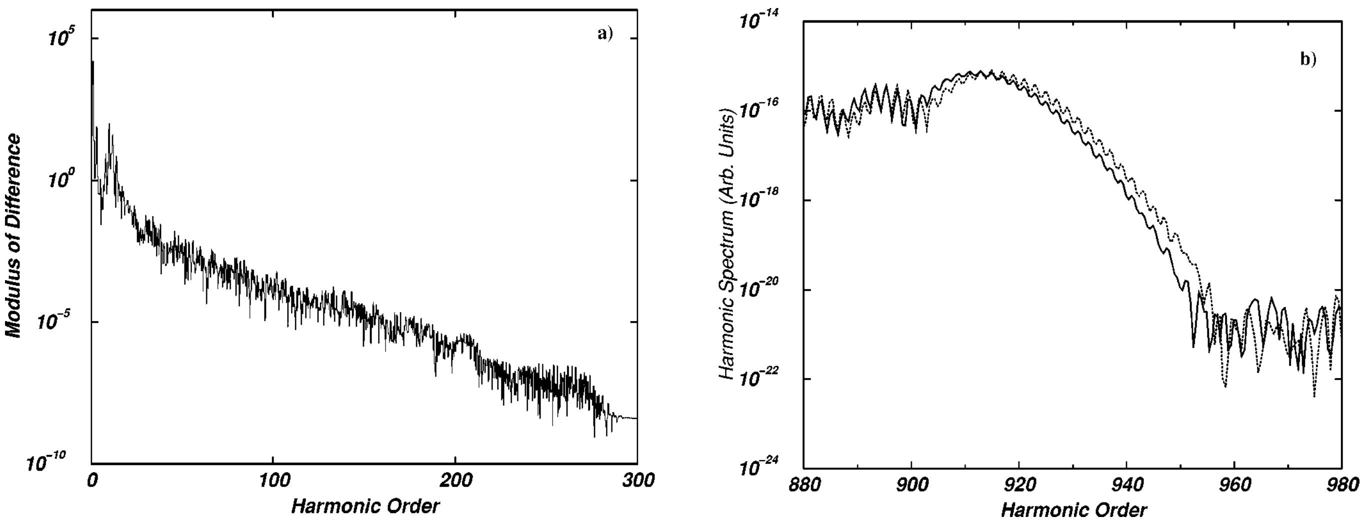

FIG. 8. (a) The modulus of the difference of the spectrum, which is polarized in the *x* direction and calculated via the Pauli equation (30), with the analogous one, which is calculated via Eq. (38), is depicted. The laser parameters are $I=5.932\times10^{16}$ W/cm^2, $\lambda=248$ nm with a turn-on phase of five cycles and a duration of the phase with constant amplitude of five cycles. (b) Segment of the spectrum near the cutoff regime of the *x*-polarized harmonic spectra via the Pauli equation (30) (dashed line) and via Eq. (38), i.e., including spin-orbit coupling (solid line). The laser parameters are $I=2.36\times10^{17}$ W/cm^2, $\lambda=248$ nm with a turn-on phase of one cycle, and a duration of the phase with constant amplitude of two cycles.

We thus note that the relative direct radiation via spin dynamics is quite small in total and likely to be difficult to detect via current laser intensities. The promising way around this would be at present the detection of *y* polarized light as described in the previous subsection.

2. Spin-induced radiation

As noted in Sec. IV B, the spin dynamics modifies the electron dynamics and with this also the probability of the electron recombination during the HHG process, i.e., the intensity of the HHG. The following estimations shall give an idea of necessary laser intensities when these effects become large. We may say that spin effects disturb the dynamics of the electron substantially when additional spin terms in the Hamiltonian ΔH_s are of the order of the characteristic energy of the process itself. In the considered case of HHG via tunneling ionization the characteristic energy is $|\epsilon_p-\epsilon_i|\approx\epsilon_p$, where $\epsilon_p=-2\sqrt{Ze^3E}$ is the maximal value of the total potential surface of the ion and the laser field and

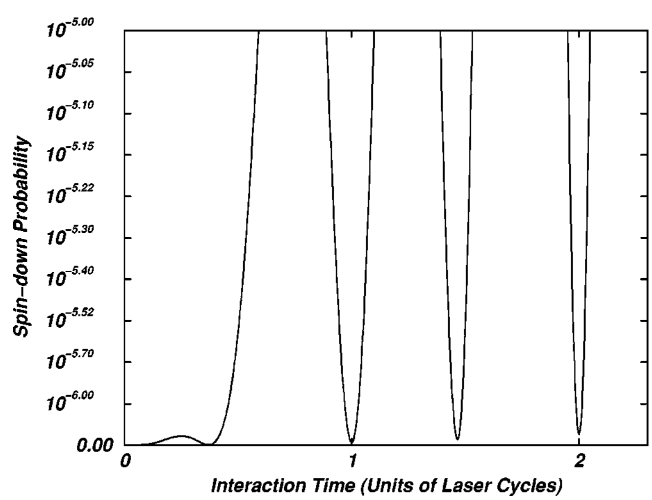

FIG. 9. The spin-down population of the wave function as a function of time. The spin-orbit coupling causes an effective polarization of the spin, while without spin-orbit coupling the electron returns periodically to the initial polarization in complete spin-up configuration (see, e.g., Fig. 5). The parameters are the same as in Fig. 8(a).

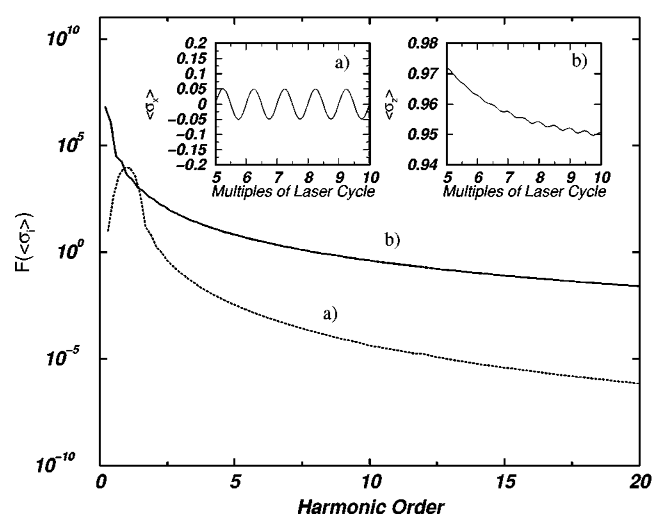

FIG. 10. The insets (a) and (b) show the expectation values of σ_x and σ_z as a function of time in laser cycles, respectively. Here, $\boldsymbol{\mu}=(e\hbar/2mc)\langle\boldsymbol{\sigma}\rangle$ with $\boldsymbol{\mu}$ given in Eq. (42). In the main part of the figure, the dotted curve $F(\langle\sigma_x\rangle)$ is the Fourier transform of $\langle\sigma_x\rangle$ and is thus associated with inset (a), whereas the solid curve $F(\langle\sigma_z\rangle)$ with association (b) is the Fourier transform of $\langle\sigma_z\rangle$. The laser parameters involve an intensity $I=5.9320\times10^{16}$ W/cm^2, a wavelength $\lambda=248$ nm, and a pulse shape with five cycles turn-on phase and five cycles maximal amplitude.

$-\epsilon_i$ is the ionization energy. ΔH_s involves the characteristic energies $(e\hbar/2mc)\boldsymbol{\sigma}\cdot\boldsymbol{B}$ and $(\hbar/4m^2c^2r)(d\Phi/dr)\boldsymbol{L}\cdot\boldsymbol{\sigma}$ which are of order $\zeta\hbar\omega$ and $\zeta^2\hbar\omega$, respectively ($\boldsymbol{L}$ and $\boldsymbol{\sigma}$ are the angular momentum and spin vectors). In estimating the spin-orbit term we have assumed that the characteristic distance is $\sqrt{Ze^2/eE}$ which equals the distance from the nucleus to the point in space at which the total potential of the laser field and the ion is peaked. As a consequence, the condition for spin effects to play a large role is $\Delta H_s \approx \zeta^2\hbar\omega \approx |\epsilon_p|$, i.e.,

$$\zeta \approx (Z\alpha mc^2/\hbar\omega)^{1/3}, \tag{46}$$

where $\alpha = e^2/\hbar c$. Thus, for laser intensities starting at 10^{21} W/cm^2, spin-induced dynamics stops being a correction to become a crucial element of tunneling recollision dynamics.

We finally estimate the role of spin induced dynamics via laser electron interaction, as considered in Sec. II B, for the situation of bound electrons in intense laser fields. From Eq. (A7) we note that the kind of spin reaction discussed in Sec. II results in an electron oscillation along the magnetic-field direction with order of magnitude $\delta y \approx E_0 M/mc\omega$ with $M = e\hbar/2mc$. We may say this oscillation is large on the scale of an atomic system when $\delta y \approx a_B$, where a_B is the Bohr radius. In this case the electron drift shall affect the electron recombination probability in the situation of tunneling recombination dynamics of interest here substantially. This condition leads to the following criteron:

$$\zeta \approx 1/\alpha Z. \tag{47}$$

Thus, for highly charged ions, the effect of spin reaction studied for free electrons in Sec. II B shall be rather large for bound electrons.

V. CONCLUSION

The role of the spin degree of freedom of a free-electron, a scattered-electron and a single-electron ion in an intense low-frequency laser pulse has been investiagted with respect to dynamics and radiation. The free electron as expected is generally well described without the spin. However, for the particular motion in the laser magnetic-field direction, which would be absent without the spin, a characteristic spin-induced oscillation was identified within an efficient approach. In the scattering scenario of a laser-dressed electron at a nucleus we calculated the amount of spin dynamics as a function of the setup and the laser and ion parameters. The spin may be turned substantially only for very small impact parameters. Most attention was paid to the single-electron ion Be^{3+} in such an intense laser field where tunnel-recollision dynamics occurs and high-order harmonic generation is appreciable. The dynamics was described with an equation of motion arising from an expansion of the Dirac equation to the second order in the ratio of the velocity of the electron and the speed of light, i.e., including the coupling of the spin to the laser magnetic field in first order and the angular momentum of the electron in second order. In terms of spin signatures, pure spin radiation and narrow high-frequency harmonics were identified due to spin-induced oscillations and a small shift of the cutoff and an effective spin polarization due to second-order relativistic effects with spin. As compared to the relativistic multiphoton regime [19], the size of the effects is generally smaller in the tunneling regime for comparable laser parameters and thus smaller ion charges. Analytical estimations of the order of magnitude of spin effects showed that they become generally large only at rather high-laser intensities.

ACKNOWLEDGMENTS

We are funded by the German Science Foundation (Nachwuchsgruppe within SFB 276). M.W.W. was partly supported by the Austrian Academy of Sciences. C.H.K. acknowledges discussions with C. Szymanowski at the onset of the project.

APPENDIX: SPIN-INDUCED DYNAMICS OF FREE ELECTRONS IN LASER FIELDS

We now turn to calculation of spin reaction and develop a classical theory in four-notation which is equivalent to that provided in [10], whereas however an implicit analytical solution of the equation of motion is possible and thus can be compared with earlier quantum-mechanical results [11]. To this end we introduce the four-vector M which is dual to the tensor μ describing the spin [10], i.e.,

$$\mu_{\alpha\beta} = \frac{1}{c}\epsilon_{\alpha\beta\gamma\delta}u^{\gamma}M^{\delta}, \quad M^{\alpha} = \frac{1}{2c}\epsilon^{\alpha\beta\gamma\delta}u_{\beta}\mu_{\gamma\delta}. \tag{A1}$$

The quantities M and μ are explicitely determined by each other. From the equation for μ [21],

$$\frac{1}{\kappa}\dot{\mu}_{\alpha\beta} = \mu_{\alpha\gamma}F^{\gamma}_{\beta} - \mu_{\beta\gamma}F^{\gamma}_{\alpha}, \tag{A2}$$

we derive an equation for M^{α} by means of Eq. (A1) using the here approximate relation for spinless particles $\dot{u}^{\alpha}, = \kappa F^{\alpha\beta}u_{\beta}$,

$$\dot{M}^{\alpha} = \kappa F^{\alpha\beta}M_{\beta}. \tag{A3}$$

This is the Bargmann-Michel-Telegdi (BMT) equation [24]. The relation $\dot{u}^{\alpha} = \kappa F^{\alpha\beta}u_{\beta}$ is also used in deriving the BMT equation itself [24]. Conversely, it is demanding but possible to show that equation (A2) follows from Eq. (A3). Thus Eqs. (A3) and (A2) are equivalent.

Using Eq. (A1) the Lagrange function [10] reads

$$\mathcal{L} = \frac{mc^2}{\gamma} - \frac{1}{2c\gamma}\epsilon_{\alpha\beta\gamma\delta}u^{\gamma}M^{\delta}F^{\alpha\beta} + \frac{q}{c}A_{\alpha}v^{\alpha}. \tag{A4}$$

In the case of a linearly polarized plane laser field $\boldsymbol{E} = (E = E_0\cos(kx),0,0)$, $\boldsymbol{B} = (0,E,0)$ the BMT equation writes

$$\frac{dM^0}{d\tau} = -\frac{eE}{mc}M_1, \quad \frac{dM^1}{d\tau} = \frac{eE}{mc}(M_0 + M_3),$$

$$\frac{dM^2}{d\tau}=0,\quad \frac{dM^3}{d\tau}=-\frac{eE}{mc}M_1. \tag{A5}$$

M^2 and $\mathfrak{M}=M^0-M^3$ are constants of motion and for convenience we employed the four vector product kx, where k stands for $(\omega,\vec{k})$ with wave-vector $\vec{k}$ and x stands for $(t,\vec{r})$ with spatial vector $\vec{r}$ in this appendix. From Eq. (A4) we derive the equations of motion for the particle,

$$\frac{du^0}{d\tau}=-\frac{qE}{mc}u_1+\frac{E_0}{mc}M^2\frac{d}{d\tau}\cos(kx)+\frac{\omega E_0}{mc^2}[u_2\mathfrak{M}+(u_0+u_3)M^2]\sin(kx),$$

$$\frac{du^1}{d\tau}=\frac{qE}{mc}(u_0+u_3),\quad \frac{du^2}{d\tau}=\frac{E_0}{mc}\mathfrak{M}\frac{d}{d\tau}\cos(kx),$$

$$\frac{du^3}{d\tau}=-\frac{qE}{mc}u_1+\frac{E_0}{mc}M^2\frac{d}{d\tau}\cos(kx)+\frac{\omega E_0}{mc^2}[u_2\mathfrak{M}+(u_0+u_3)M^2]\sin(kx). \tag{A6}$$

With regard to initial conditions we assume now that the particle has zero velocity when the complete radiation pulse is still far away from the particle (vanishing vector potential at the particle). In this way we can be certain that whatever velocity the particle has at later times will be solely due to the interaction with the pulse. We also impose that in the beginning the particle is located at the origin, therefore $\eta=\omega\tau$. Then subtracting the first equation in Eqs. (A6) from the last one, it follows that $\mathfrak{u}:=u^0-u^3$ is constant. Integration over the proper time τ leads to $\eta=\omega t-kz=k\mathfrak{u}\tau-kz(0)$. We can require now for all $i\in\{0,1,2,3\}$ that $u^i(\eta)\to 0$ for those η for which $\boldsymbol{A}(\eta)\to 0$. For the vector potential $\boldsymbol{A}$ we assume that $\boldsymbol{A}(\eta)=(A=-E_0/k\sin(\eta),0,0)$ if $\eta_{\min}\leqslant\eta\leqslant\eta_{\max}$ and $\boldsymbol{A}(\eta)=(A=0,0,0)$ otherwise. We choose $\eta_0=-\infty$ to be the initial instant. Independent of the special initial conditions the equation for $u^2(\eta)$ writes

$$\frac{du^2}{d\eta}=\frac{E_0}{mc}\mathfrak{M}\frac{d}{d\eta}\cos(\eta). \tag{A7}$$

M and the spin S are connected via $M=\kappa S,\quad \kappa=q/mc$ [24]. The relation between the spin s in the rest frame of the particle and S is

$$S_0=\frac{\boldsymbol{u}}{c}\cdot\boldsymbol{s},\quad \boldsymbol{S}=\boldsymbol{s}+\frac{1}{\gamma+1}\left(\frac{\boldsymbol{u}}{c}\cdot\boldsymbol{s}\right)\frac{\boldsymbol{u}}{c}.$$

In the rest frame we suppose $\boldsymbol{s}^2=\hbar^2/4$. We choose $s^1(0)=s^2(0)=0$ and $s^3(0)=\hbar/2$. Thus, we get for the velocity u^2 and the acceleration a^2 in y direction

$$u^2(\eta)=-\frac{q\hbar E_0}{2m^2c^2}\cos(\eta),$$

$$a^2(\eta)=\frac{q\hbar E_0\omega}{2m^2c^2}\sin(\eta), \tag{A8}$$

which is the result shown in Eq. (18). This means that up to a factor 1/2 which can be associated with the Thomas precession classical and quantum-mechanical results coincide as far as the additional acceleration in y direction is concerned [11]. We note that there are certainly also influences of the spin on the dynamics in the other two directions. However, those deviations are likely to be more challenging to implement experimentally at least in the weakly relativistic regime because there is already significant dynamics in those directions without a spin degree of freedom.

[1] *Atoms in Intense Laser Fields*, edited by M. Gavrila (Academic, San Diego, 1992); M. Protopapas, C. H. Keitel, and P. L. Knight, Rep. Prog. Phys. **60**, 389 (1997); C. J. Joachain, M. Dörr, and N. Kylstra, Adv. At. Mol. Phys. **42**, 225 (2000); T. Brabec and F. Krausz, Rev. Mod. Phys. **72**, 545 (2000).

[2] B. W. Shore and P. L. Knight, J. Phys. B **20**, 413 (1987); J. L. Krause, K. J. Schafer, and K. C. Kulander, Phys. Rev. Lett. **68**, 3535 (1992); P. B. Corkum, *ibid.* **71**, 1994 (1993); W. Becker, S. Long, and J. K. McIver, Phys. Rev. A **41**, 4112 (1990); **50**, 1540 (1994); A. L'Huillier and P. Balcou, Phys. Rev. Lett. **70**, 774 (1993); J. J. Macklin, J. D. Kmetec, C. L. Gordon III, and S. E. Harris, *ibid.* **70**, 766 (1993). M. Lewenstein *et al.*, Phys. Rev. A **49**, 2117 (1994); M. Protopapas *et al.*, *ibid.* **53**, R2933 (1996); G. van de Sand and J. M. Rost, Phys. Rev. Lett. **83**, 524 (1999).

[3] Ch. Spielmann *et al.*, Science **278**, 661 (1997); M. Schnürer *et al.*, Phys. Rev. Lett. **80**, 3236 (1998); Ch. Spielmann *et al.*, IEEE Antennas Propag. Mag. **4**, 249 (1998); G. Tempea, M. Geissler, and T. Brabec, J. Opt. Soc. Am. B **16**, 669 (1999); G. Tempea *et al.*, Phys. Rev. Lett. **84**, 4329 (2000).

[4] Z. H. Chang *et al.*, Phys. Rev. Lett. **79**, 2967 (1997); A. Rundquist *et al.*, Science **280**, 1412 (1998); H. Kapteyn and M. Murnane, Phys. World **12**, 31 (1999); C. G. Durfee III *et al.*, Phys. Rev. Lett. **83**, 2187 (1999); R. Bartels *et al.*, Nature (London) **406**, 164 (2000).

[5] P. H. Mokler and Th. Stoehlker, Adv. At. Mol. Phys. **37**, 297 (1996); J. Ullrich *et al.*, J. Phys. B **30**, 2917 (1997); T. Ditmire *et al.*, Phys. Rev. A **57**, 369 (1998).

[6] S. J. McNaught, J. P. Knauer, and D. D. Meyerhofer, Phys. Rev. A **58**, 1399 (1998); V. P. Krainov, J. Phys. B **32**, 1607 (1999); R. Taïeb, V. Véniard, and A. Maquet, Phys. Rev. Lett. **87**, 053002 (2001).

[7] S. E. Harris, Phys. Rev. Lett. **31**, 341 (1973); S. Kubodera *et al.*, Phys. Rev. A **48**, 4576 (1993); S. G. Preston *et al.*, *ibid.* **53**, R31 (1996); M. Casu *et al.*, J. Phys. B **33**, L411 (2000).

[8] L. S. Brown and T. W. Kibble, Phys. Rev. **133**, A705 (1964); E. S. Sarachik and G. T. Schappert, Phys. Rev. D **1**, 2738 (1970); A. I. Nikishov, and V. I. Ritus, Zh. Éksp. Teor. Fiz. **46**,

776 (1964) [Sov. Phys. JETP **19**, 529 (1964)]; I. I. Goldman, *ibid.* **46**, 1412 (1964) [*ibid.* **19**, 954 (1964)]; W. Becker, J. Phys. A **9**, 149 (1976).
[9] C. I. Moore, J. P. Knauer, and D. D. Meyerhofer, Phys. Rev. Lett. **77**, 2335 (1996); C. Bula *et al.*, *ibid.* **76**, 3116 (1996); C. H. Keitel *et al.*, J. Phys. B **31**, L75 (1998); S. Y. Chen, A. Maksimchuck, and D. Umstadter, Nature (London) **396**, 653 (1998); J. San Roman, L. Roso, and H. R. Reiss, J. Phys. B **33**, 1869 (2000); S.-Y. Chen *et al.*, Phys. Rev. Lett. **84**, 5528 (2000).
[10] M. W. Walser, C. Szymanowski, and C. H. Keitel, Europhys. Lett. **48**, 533 (1999).
[11] M. W. Walser and C. H. Keitel, J. Phys. B **33**, L221 (2000).
[12] J. Grochmalicki, M. Lewenstein, and K. Rzazewski, Phys. Rev. Lett. **66**, 1038 (1991); T. Katsouleas and W. B. Mori, *ibid.* **70**, 1561 (1993); C. H. Keitel and P. L. Knight, Phys. Rev. A **51**, 1420 (1995); M. Protopapas, C. H. Keitel, and P. L. Knight, J. Phys. B **29**, L591 (1996); N. J. Kylstra, A. M. Ermolaev, and C. J. Joachain, *ibid.* **30**, L449 (1997); R. Taïeb, V. Véniard, and A. Maquet, Phys. Rev. Lett. **81**, 2882 (1998); S. X. Hu and C. H. Keitel, Europhys. Lett. **47**, 318 (1999); J. R. Vázquez de Aldana and Luis Roso, Opt. Express **5**, 144 (1999); R. M. Potvliege, Laser Phys. **10**, 143 (2000); H. R. Reiss, Phys. Rev. A **63**, 013409 (2000); N. J. Kylstra *et al.*, Phys. Rev. Lett. **85**, 1835 (2000).
[13] C. H. Keitel, P. L. Knight, and K. Burnett, Europhys. Lett. **24**, 539 (1993); C. Szymanowski, C. H. Keitel, and A. Maquet, Laser Phys. **9**, 133 (1999); J. C. Csesznegi *et al.*, *ibid.* **9**, 41 (1999); R. E. Wagner, R. J. Reverly, Q. Su, and R. Grobe, Phys. Rev. A **60**, 3233 (1999); D. J. Urbach and C. H. Keitel, *ibid.* **61**, 043409 (2000); M. W. Walser *et al.*, Phys. Rev. Lett. **85**, 5082 (2000); R. M. Potvliege, N. J. Kylstra, and C. J. Joachain, J. Phys. B **33**, L743 (2000); D. B. Milošević, S. X. Hu, and W. Becker, Phys. Rev. A **63**, 011403(R) (2001); N. J. Kylstra, R. M. Potvliege, and C. J. Joachain, J. Phys. B **34**, L55 (2001); K. Z. Hatsagortsyan and C. H. Keitel, Phys. Rev. Lett. **86**, 2277 (2001); C. H. Keitel and S. X. Hu, Appl. Phys. Lett. **80**, 541 (2002).
[14] U. W. Rathe *et al.*, J. Phys. B **30**, L531 (1997).
[15] M. M. Denisov and M. V. Fedorov, Zh. Éksp. Teor. Fiz. **53**, 1340 (1967) [Sov. Phys. JETP **26**, 779 (1968)]; J. Z. Kamiński, J. Phys. A **18**, 3365 (1985); F. Zhou and L. Rosenberg, Phys. Rev. A **48**, 505 (1993); N. F. Mott, Proc. R. Soc. London, Ser. A **124**, 425 (1929); **A135**, 429 (1932); A. Weingartshofer *et al.*, Phys. Rev. Lett. **39**, 269 (1977); H. K. Avetissian *et al.*, Phys. Rev. A **59**, 549 (1999).
[16] C. Szymanowski *et al.*, Phys. Rev. A **56(5)**, 3846 (1997).
[17] J. W. Braun, Q. Su, and R. Grobe, Phys. Rev. A **59**, 604 (1999); for Dirac dynamics without laser fields see, e.g., R. Arvieu, P. Rozmej, and M. Turek, *ibid.* **62**, 022514 (2000).
[18] O. Latinne, C. J. Joachain, and M. Dörr, Europhys. Lett. **26**, 333 (1994); J. R. Vázquez de Aldana and Luis Roso, J. Phys. B **33**, 3701 (2000); M. W. Walser and C. H. Keitel, Opt. Commun. **199**, 447 (2001).
[19] S. X. Hu and C. H. Keitel, Phys. Rev. Lett. **83**, 4709 (1999); Phys. Rev. A **63**, 053402 (2001).
[20] C. H. Keitel, Contemp. Phys. **42**, 353 (2001).
[21] J. Frenkel, Z. Phys. **37**, 243 (1926); H. J. Bhabha and H. C. Corben, Proc. R. Soc. London, Ser. A **178**, 273 (1941); P. Nyborg, Nuovo Cimento **23**, 47 (1962); D. Hestenes, J. Math. Phys. **15**, 1768 (1974); M. W. Walser and C. H. Keitel, Lett. Math. Phys. **55**, 63 (2001).
[22] J. Bailey and E. Picasso, Prog. Nucl. Phys. **43**, 428 (1970).
[23] I. S. Gradshteyn and I. M. Ryzhik, *Tables of Integrals, Series and Products*, 4th ed. (Academic Press, New York, 1965).
[24] J. D. Jackson, *Classical Electrodynamics*, 2nd ed. (Wiley, New York, 1975).
[25] L. D. Landau and E. M. Lifshitz, *Mechanics*, 3rd ed. (Pergamon Press, Oxford, 1976).
[26] Paul Strange, *Relativistic Quantum Mechanics* (Cambridge University Press, Cambridge, 1998); for an alternative approach see L. L. Foldy and S. A. Wouthuysen, Phys. Rev. **78**, 29 (1950).
[27] K. C. Kulander *et al.*, in *Proceedings of the Workshop on Super-intense Laser Atoms Physics (SILAP)*, edited by B. Piraux (Plenum, New York, 1993).
[28] J. H. Eberly, Q. Su, and J. Javanainen, Phys. Rev. Lett. **62**, 881 (1998).
[29] J. A. Fleck, J. Morris, and M. D. Feit, Appl. Phys. **10**, 129 (1976).
[30] R. Heather, Comput. Phys. Commun. **63**, 446 (1991).
[31] A. Bandrauck and H. Shen, Chem. Phys. Lett. **176**, 428 (1991).
[32] M. D. Feit, J. A. Fleck, and A. Steiger, J. Comput. Phys. **47**, 412 (1982).